

# DESIGNING THE EUROPEAN SPALLATION SOURCE TUNING DUMP BEAM IMAGING SYSTEM\*

M. G. Ibison<sup>†</sup>, C. P. Welsch, Cockcroft Institute and University of Liverpool, Warrington, UK  
 E. Adli, G. Christoforo, H. Gjersdal, University of Oslo, Oslo, Norway  
 T. J. Shea, C. A. Thomas, ESS, Lund, Sweden

## Abstract

The first section of the European Spallation Source (ESS) to receive high-energy protons when live operation begins will be the Tuning Dump beam-line. The dump line will be used during accelerator commissioning to tune the linac, and must accept the full range of ESS energies up to 2 GeV, from 5µs probe pulse to full 2.86ms pulse length, and beam sizes up to the 250 mm limit of the physical aperture, although the allowed pulse rate will be restricted by the thermal capacity of the dump. An imaging system has been developed to view remotely the transverse beam profile in the section immediately before the dump entrance, using insertable scintillator screens. This contribution presents the principal design parameters for this system, with particular reference to the techniques used in assessing the radiation and thermal environments and their impact on the selection of locations for the imaging cameras, and the specification of the mechanical screen actuators. The predicted optical performance of the system is also summarised.

## SYSTEM REQUIREMENT FOR TUNING DUMP IMAGING

The Tuning Dump (TD) receives the ESS beam during initial commissioning and LINAC tune-up, to study the beam without its reaching the target. The dump can safely handle short proton pulses, or reduced rate full pulses [1].

Imaging of the beam transverse profile will be provided in at least two locations upstream of the dump, their longitudinal separation enabling beam divergence measurement. A beam to be imaged may occupy any part of the full physical exit aperture. The main parameters constraining the system are listed in Table 1.

Table 1: TD System Requirements - Principal Parameters

Parameter	Value	Origin
Field of View	Max poss	Full beam-pipe dia 250 mm
Limiting Apertures	200 mm 120 mm	Vessel viewports Camera penetration*
Beam Size (nominal)	1.6 cm (rms)	Beam dynamics simulation [1]
Resolution	≤1 mm	Beam profile
Max Average Power	12.5 kW	Use Case: 'Slow Tuning Beam' [1]

\*see Final Design (later)

## DESIGN APPROACH

After considering curved-mirror systems or optical fibres with remote cameras, the final design has a simple 'periscope' configuration with 2 plane mirrors, combining acceptable image quality and flexible camera positioning. The components, which are modelled in the optical design software ZEMAX OpticStudio [2], therefore include:

- the object (screen intercepting proton beam)
- the viewport in the vacuum vessel
- 1<sup>st</sup> 45° mirror (outside the viewport)
- 2<sup>nd</sup> 45° mirror (on ray-path from 1<sup>st</sup> mirror)
- imaging lens and camera

The primary light source for TD imaging will be a 'Chromox' ceramic screen, excited into photon emission by the energetic incident protons; studies are also ongoing into improved materials with adequate photon yield, spectrum, lifetime & linearity which preserve their properties after the heat of the spraying process used in application.

## STUDIES OF RADIATION AND THERMAL ENVIRONMENT

The dump line imaging vessels, the dump and its shielding have been modelled in the Monte-Carlo radiation transport code FLUKA [3], to find positions for the cameras providing the required field of view while giving a useful lifetime before radiation damage to the sensor compromised the image quality. Based on other studies [4], a dose target has been set at 20 Grays/year for selecting an imaging camera location, to minimise degradation.

### Camera Radiation Dose

For the TD system, absorbed dose was recorded in regions proposed for the imaging cameras. Dose is estimated from the FLUKA score per primary particle and the total number calculated from the projected beam current and annual beam-on-dump time, based on the equation:

$$\begin{aligned} \text{Protons per year} &= 0.5 \times t_s \times 3600 \times \frac{I_P}{e} \\ &= 3.54 \times 10^{19} \end{aligned}$$

where annual machine study time  $t_s = 500$  h; time-on-dump fraction (estimated) = 0.5; beam current (mean)  $I_P = 6.3 \mu\text{A}$ ;  $e =$  electronic charge.

Most of the camera dose in Table 2 has been shown to be due to particle scatter from the imaging screen, plus some radiation escaping from the dump entrance.

\*Work supported by In-Kind Agreements, ESS/UK, ESS/Norway

<sup>†</sup> mark.ibison@cockcroft.ac.uk

Exploring new locations, the FLUKA model was developed in stages, adding further geometry; doses at multiple camera positions could be compared in the same run.

Table 2: Camera Doses for Selected Locations

Location	Camera 1	Camera 2
<i>INITIAL</i> Shielded Bunker on Tunnel Floor, 5cm concrete lid	700 ± 150	380 ± 90
<i>INTERMEDIATE</i> High-Level, unshielded	100 ± 150	40 ± 70
<i>FINAL</i> High-Level, in 1.5m hole	N/A	undetectable

Cameras 1 & 2 to L & R sides. Doses in Gy/yr; errors ±1σ

### Dose from Lost Particles

In ESS 'User' mode, the beam from the LINAC enters the target line via dipole magnets in the first 'dog-leg' bend shown in Fig.1. Protons lost from the beam hereabouts can enter the dump tunnel, adding to the total dose to the imaging cameras.

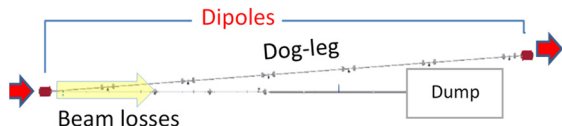


Figure 1: Beam losses from first dipole in the dog-leg section, which enter the dump tunnel. Beam from LINAC enters from L, beam to target leaves to R.

Earlier ESS modelling provided input data files of full parameters (position, direction and energy) for a large particle set. Code was written to read the prepared data into the existing TD FLUKA model. The dose per proton at the camera, and hence the total annual dose, was obtained using the result:

$$\begin{aligned}
 & \text{Proton Losses to Dump Tunnel per year} \\
 &= (5300 \times 3600) \times (2.52 \times 10^{-3}) \\
 &\quad \times (0.002 \times 0.01) / e \\
 &= 6.00 \times 10^{18} \text{ protons}
 \end{aligned}$$

where average beam current (5MW full power beam on target) = 2.52mA, operating hours = 5300 per year, and fractional loss rate at the dipole = 0.002% (assumed).

Particle loss doses to the camera in the final location selected were undetectable in FLUKA simulations.

### Dose-Rates from Decay

Dose-rates at the imaging station near the TD just after beam shut-off, due to activation product decay in the dump region, were studied; the ESS Operation Schedule gave the expected beam-on-dump timings after start-up.

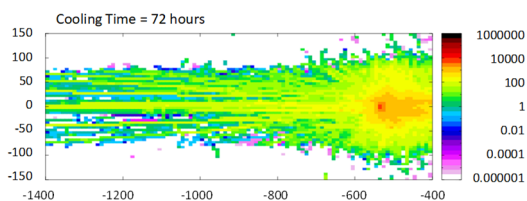
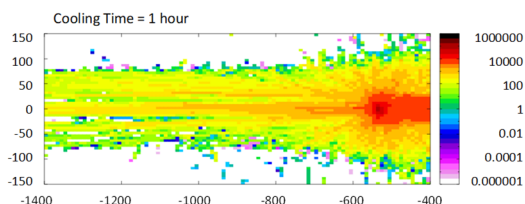


Figure 2: Decay dose-rate plots in horizontal beam plane near the imaging vessel, after 1 & 72 hours' cooling time. Distances in cm, dose-rate in μSv/h.

FLUKA inputs particle irradiation times and rates, and outputs dose-rate at selected decay times after beaming. The dose-rate profile in the horizontal beam plane was plotted as shown in Fig.2, 1 to 72 hrs post shut-down, after 1 year's operation.

In addition, an independent analytical study calculated the activity induced by a 4.5cm radius beam of 2GeV protons via Cu(p,xn) reactions [5] in the copper dump cylinder followed by decay of the 21 most important nuclides produced. The dose-rate 4m from this source on the beam axis (the approximate location of the imaging vessel), was then estimated for each significant gamma-ray [6]. A 'geometry factor' for a cylindrical source, derived from an expression in its radius and height, and the distance from its centre on axis, was applied [7], and the contributions summed for the total dose-rate. The results shown in Table 3 are consistent, given uncertainties; the analytical approach ignores dump self-shielding, and at shorter cooling, FLUKA data is enhanced by rapid-decay radiation from the screen.

Table 3: Decay Dose Rates From Estimation Methods

Cooling Time (hours)	1	72
Total Dose-Rate (analytical)	51.3	20.6
Dose-Rate (from FLUKA)	10-100	1-10

All dose-rates are quoted in mSv/hr.

### Screen Heating Studies

Studies have been made on the instantaneous heating by a single full ESS proton pulse passing through the imaging screen, assuming no immediate heat removal, as in Fig.3.

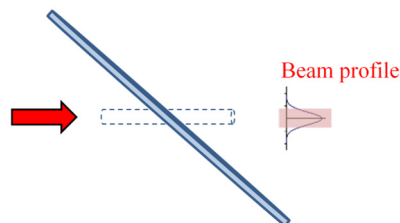


Figure 3: Model of passage of beam through screen, showing 'core' region for thermal analysis (1σ width).

In Fig.4, the peak temperature reached in the layers of a composite screen is plotted against beam size (at 1σ), assuming a Gaussian distribution. Beam 'core' regions (1σ) of the layers are considered thermally isolated from the outside. In the final design (see Fig.6), the beam is orthogonal to the screen but the heat deposited per unit

Content from this work may be used under the terms of the CC BY 3.0 licence (© 2019). Any distribution of this work must maintain attribution to the author(s), title of the work, publisher, and DOI

volume is still approximately the same.

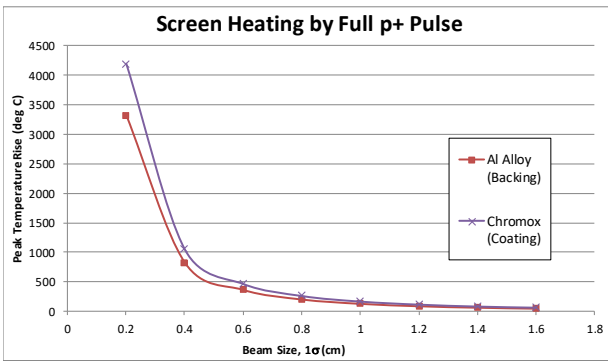


Figure 4: Peak temperature in screen layers vs. beam size, for one full pulse of  $1.114 \times 10^{15}$  protons, at  $E_p = 570$  MeV.

Results indicate that a coated Al-alloy screen (melting pt (MP)  $\sim 580^\circ\text{C}$ ) is safe to beam size  $\sigma_x \geq 0.75$  cm, but Chromox (MP  $\sim 2000^\circ\text{C}$ ) could be used at  $\sigma_x \geq 0.4$  cm. In comparison, a nominal beam of size  $\sigma_x = 1.6$  cm is predicted to heat the screen materials by up to only  $70^\circ\text{C}$ .

## DESCRIPTION OF FINAL SYSTEM

Initially, two identical systems will be installed, with provision for a third at a set upstream location, as Fig.5 indicates; access to three profiles would enable more advanced diagnostics, including emittance measurements.

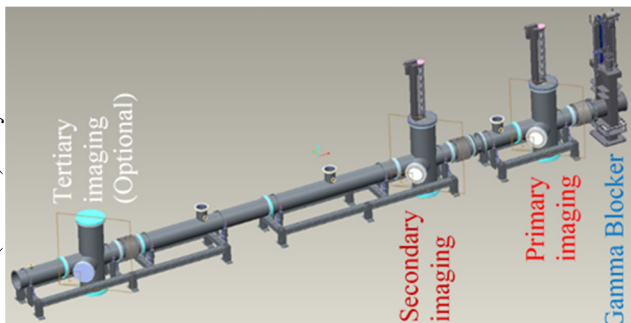


Figure 5: Locations of imaging stations in the dump line. Tertiary imaging vessel is to be initially installed empty. Beam direction is from bottom L to top R.

In Fig.6, each imaging vessel is a special 5-way cross, horizontal arms suiting the 250 mm beam-pipe, but 350 mm verticals take wider screens to cover the full aperture. Beam-height is 500 mm above the floor, giving space below for the vessel to accept one unused screen in its lower vertical, and tall enough above to take both screens raised clear of the beam. Maintenance is eased by clamping with threaded half-rings rather than nuts at the top and viewport flanges of the vessel, also allowing rotatability.

A long-travel vertical linear actuator on the top flange, with edge-welded bellows and lead-screw, moves one of 2 screens into the beam. The ‘harsh-environment’ motor will drive an in-line gearbox or may be directly-coupled if higher-rated. Drive-belts are avoided due to radiation-dose failure risk. All motion control is by five limit switches: intermediate screen positions and end-of-travel.

Screens mounted at  $90^\circ$  to the beam are viewed through a 200 mm fused-quartz viewport on the  $45^\circ$  arm. The

window may be changed when transmission falls; quartz resists radiation, but a dose of  $\leq 5.7$  kGy/year is predicted.

Images will pass vertically, by twin  $45^\circ$  plane mirrors, to cameras in 1.5m holes drilled in the tunnel walls, 1.5m above the beam. Remotely-controlled lenses will focus the final images and adjust the  $f$ -number in Table 4. Remote filter-changers just before the lens, or at the shield-wall entrance leading to the camera, select attenuation for intensities saturating the camera. Depth-of-field across the full screen width may be improved with a tilt of  $<2^\circ$  to the camera sensor, by the Scheimpflug principle [8].

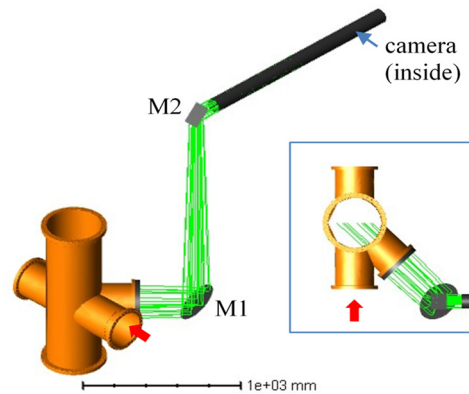


Figure 6: Optical path from a screen inside the vessel, via plane mirrors to a camera located inside a hole drilled into the shield wall. Proton beam direction is indicated by the red arrow. (Inset: Plan view, with beam from bottom.)

Table 4: Optics Design Parameters for the TD System

Parameter	TD system
Focal Length (mm) – set by lens selected	135
$f/\#$ {proposed}	$f/2.85 \{f/2\}^\dagger$
Mirrors: Clear Diameter (mm)	M1 290 M2 110 x 150
Screen – Lens Distance (mm)	3828*

\*variable, depending on exact position of camera

$\dagger$  depends on position & hole diameter (see Fig.6)

## CONCLUSION

A simplified optical system has been designed to image the ESS proton beam in the Tuning Dump line. Developed and optimised using the Zemax toolset, it meets performance requirements under severe radiation environment conditions. Prototyping with the specified mirrors/lens has shown that they meet imaging requirements.

Assessing radiation dose in the Dump line after irradiation has informed the location of cameras to give adequate life, materials choice for other key components, and expected conditions during maintenance access. A vacuum vessel and mechanical elements detailed design has been developed, meeting vacuum and other requirements.

Designing for resilience and durability has assured longevity with maintainability. This type of imaging system would suit other high-power proton beamlines, unless a non-invasive diagnostic is required. The risk of screen damage from the beam, breakage or loss of emission, is mitigated with a running spare at each imaging station.

## REFERENCES

- [1] Y. Lee *et al.*, “Working Concept of 12.5 kW Tuning Dump at ESS”, in *Proc. 8th Int. Particle Accelerator Conf. (IPAC'17)*, Copenhagen, Denmark, May 2017, pp. 4591-4594. doi:10.18429/JACoW-IPAC2017-THPVA065
- [2] ZEMAX LLC, Kirkland, WA 98033 USA, <http://www.zemax.com/os/opticstudio>
- [3] A. Ferrari *et al.*, “FLUKA: a multi-particle transport code”, CERN-2005-10, INFN/TC\_05/11, SLAC-R773, 2005.
- [4] S. Hutchins, M. Facchini, E. Tsoulou, “Radiation Tests on Solid State Cameras for Instrumentation”, in *Proc. DIPAC 2005*, Lyon, France
- [5] R. Michel, M. Gloris, H.-J. Lange *et al.*, “Nuclide production by proton-induced reactions on elements ( $6 \leq Z \leq 29$ ) in the energy range from 800 to 2600 MeV”, *Nuclear Instruments and Methods in Physics Research B* 103 (1995) 183-222.
- [6] “Dose Calculations: Absorbed Dose from a charged particle beam”, MIT Course in Nuclear Engineering, Principles of Radiation Interactions 22.55 (2004).
- [7] Ana Neacsu, Mihail Contineanu, Traian Zaharescu, Iulia Contineanu, “Calculation of the Gamma Radiation Dose Produced by a Cylindrical Radioactive Source”, REV. CHIM. (Bucharest) 67, No. 9, 2016.
- [8] T. Scheimpflug, “Improved Method and Apparatus for the Systematic Alteration or Distortion of Plane Pictures and Images by Means of Lenses and Mirrors for Photography and for other purposes”, UK Patent No. 1196, Jan 1904.